Published in final edited form as:
Med Dosim. 2010 ; 35(4): 297–303. doi:10.1016/j.meddos.2009.09.004.

On the use of Hyperpolarized Helium MRI to define Ventilation Volumes for Conformal Avoidance Lung Radiotherapy Treatment Planning and Delivery

C. W. Hodge[*], **W. A. Tomé**[*,#], **S. B. Fain**[#], **S. M. Bentzen**[*,#], and **M. P. Mehta**[*]

[*] University of Wisconsin, Department of Human Oncology

[#] University of Wisconsin, Department of Medical Physics

Abstract

Purpose—To illustrate the feasibility of using hyperpolarized helium MRI (HPH-MRI) to obtain functional information which may assist in improving conformal avoidance of ventilating lung tissue during thoracic radiotherapy.

Methods and Materials—HPH-MRI images were obtained from a volunteer patient. These images were first fused with a proton density weighted (PD_w) MRI to provide corresponding anatomic detail, then with the treatment planning CT of a patient from our treatment planning database who possessed equivalent thoracic dimensions. An optimized treatment plan was then generated using the TomoTherapy TPS, designating the HPH enhancing regions as Ventilation Volume (VV). A dose volume histogram compares the dosimetry of the lungs as a paired organ, the VV, and the lungs minus the VV. The clinical consequence of these changes were estimated using a bio-effect model, the parallel architecture model or local damage (f_{dam}) model. Model parameters were chosen from published studies linking the incidence of grade 3+ pneumonitis with dose and volume irradiated.

Results—For two hypothetical treatment plans of 60 Gy in 30 fractions delivered to a right upper lobe lung mass, one utilizing and one ignoring the Ventilation Volume as an avoidance structure, the NTD_{mean} values for the lung subvolumes were as follows: lungs=12.5 Gy_3 vs 13.52 Gy_3, Ventilation Volume=9.94 Gy_3 vs 13.95 Gy_3, and lungs minus ventilation volume= 16.69 Gy_3 vs 19.16 Gy_3. Using the f_{dam} values generated from these plans, one would predict a reduction of the incidence of Grade 3+ radiation pneumonitis from 12% to 4% when compared with a conventionally optimized plan.

Conclusion—The use of HPH-MRI to identify ventilated lung subvolumes is feasible, and has the potential to be incorporated into conformal avoidance treatment planning paradigms. A prospective clinical study evaluating this imaging technique is being developed.

Keywords

Lung cancer; functional imaging; radiotherapy; image guidance; magnetic resonance imaging

Corresponding Author: Professor Wolfgang A Tomé, Ph.D., University of Wisconsin Department of Radiotherapy, 600 Highland Ave, K4/314, Madison, WI 53792, Phone: 1 (608) 263-8510, Fax: 1 (608) 263-9947, tome@humonc.wisc.edu.

INTRODUCTION

Loco-regional disease progression remains a major cause of treatment failure after radiation therapy for non-small cell lung cancer (NSCLC) with 60%–80% of cases succumbing to this mode of failure. Prospective phase I/II dose escalation studies as well as a randomized controlled phase III trial have demonstrated a dose-response relationship for loco-regional control and for overall survival [1,2]. Taken together, these observations produce a strong case for intensification of radiation therapy in NSCLC. However, normal tissue side effects [3], particularly early and late lung reactions, limit the local treatment intensity. This has created interest in strategies combining radiation with cytotoxic or molecularly targeted drugs [4,5], altered dose fractionation [6,7] as well as in strategies aimed at improving radiation dose distribution, specifically as it pertains to minimizing the volume of normal lung irradiated. Refinements in image guidance and radiation delivery have served as powerful techniques for accomplishing the latter objective, as illustrated by the encouraging early clinical results observed in patients treated using hypofractionated stereotactic body radiotherapy (SBRT) for the treatment of early stage NSCLC[8–10].

Original work in functional lung imaging for treatment planning purposes focused on using lung scintigraphy, but this has not resulted in clinically meaningful applications, due to several factors including resolution limitations, relatively inaccurate image-fusion, lack of application of IMRT conformal-avoidance paradigms to treatment planning, and the issue of re-inflation/deflation of some lung volumes after treatment has been initiated[11–13]. More recently, however, novel MRI "contrast agents" have been evaluated in an attempt to improve upon the resolution afforded by lung scintigraphy [14,15]. These agents all possess a nuclear imbalance of protons and neutrons, giving them a net nuclear spin which can be exploited by MR. Gaseous elements (^{3}He and ^{129}Xe are the primary examples) have been investigated as inhaled contrast agents, with ^{3}He being especially promising due to its non-reactive nature and extremely low systemic absorption (less than 0.1%). Under normal conditions, inhaled ^{3}He has a density several thousand times less than that of hydrogen nuclei in water, and would therefore not be sufficiently concentrated to permit detection by MR. However, by *hyperpolarizing* the gas (i.e. artificially creating an increase in net polarization per unit volume) an effective contrast medium is created, allowing one to clearly visualize all airspaces which are being ventilated. Early clinical studies in a number of pulmonary diseases such as emphysema, asthma and cystic fibrosis demonstrate excellent contrast resolution of ventilatory versus non-ventilatory lung [16,17]. The images obtained using HPH-MRI can be easily cross correlated with high accuracy to treatment planning CT scans in order to transfer this functional information into conformal-avoidance IMRT planning, which has been elegantly demonstrated and validated in the study by Ireland and colleagues[18]. We report on the possible sparing of the ventilation volume (VV) as identified using HPH-MRI images employing helical tomotherapy.

MATERIALS AND METHODS

Image Acquisition and Fusion

HPH-MRI imaging of the lung was performed in a volunteer patient, using HPH administration and image acquisition techniques which have previously been described[17]. A proton density weighted (PD_w) MRI was subsequently obtained to yield anatomic detail which would allow for fusion with a treatment planning CT scan. Since the primary purpose of this study is to evaluate and explore the feasibility of preferentially sparing the ventilation volume using conformal avoidance when employing helical tomotherapy for treatment delivery we have evaluated several scans in our existing CT treatment planning database in order to selected a scan from a patient being treated for a right upper lobe lung cancer whose thoracic dimensions most closely matched those of a the volunteer patient that had undergone a HPH-MRI.

As can be seen from Figure 1 HPH-MRI is characterized by a distinct lack of anatomical information. In order to obtain highly accurate cross correlation of the HPH-MRI data to the treatment planning CT, we first fused the HPH-MRI data set to the PD_w-MRI data set that was obtained during the same imaging session, and the PD_w-MRI data set was then cross correlated to the treatment planning CT. In order to incorporate the lung subvolumes which are most ventilatory-competent into the conformal-avoidance planning process for non-small cell lung cancer, we auto-segmented these areas in the HPH-MRI data prior to image correlation, the result of which is shown in Figure 1. Finally, these volumes were projected onto the treatment planning CT, which are hereafter referred to as the Ventilation Volume (VV). (Figure 2).

Treatment Planning

After fusion with the MR images, the Pinnacle$^{3\text{™}}$ treatment planning system (Pinnacle, Philips Medical Systems, Fitchburg, WI) was used to contour all relevant structures. Upon the definition of the GTV, CTV and PTV, as well as the organs at risk (OAR), i.e. spinal cord, heart, Lungs, and the Ventilation Volume, the resulting plan was transferred to the TomoTherapy Planning System (TomoTherapy, Inc., Middleton WI) for treatment planning. The dose objectives were chosen such that the necessary normal tissue constraints for the heart and spinal cord were met in the final treatment plan. However, instead of specifying dose constraints for the Lungs, we chose to specify dose constraints for the Ventilation Volume separately, such that the resulting NTD_{mean} for the Lungs was still less than 18.5 Gy_3.

Radiobiologic Modeling

In order to estimate the potential clinical relevance of the change in dose distribution achievable by sparing of the ventilated lung volume, we applied the parallel architecture model originally proposed by Withers et al.19. This model assumes that the effect of a non-uniform radiation dose distribution is to damage some hypothetical functional subunit (FSU) with a dose dependent probability. Following, Yorke et al. 20,21, we used the parameters originally derived from Ten Haken's analysis of grade 3+ pneumonitis, that is "severe cough requiring steroids or intermittent oxygen" or worse, in patients treated at the University of Michigan (personal communication, cited in Yorke et al. 20). In this formulation, the probability of damaging a local FSU after a dose, D, is assumed to follow a logistic relationship:

$$p(D)=\frac{1}{1+\left(\frac{d_{1/2}}{D}\right)^k} \quad \text{(Eq. 1)}$$

where $d_{1/2}$=20.5 Gy and k=2.18.

The link between local damage and a resulting clinically observable side effect is also assumed to be described by a logistic function of the fraction of damaged FSU's, f_{dam}, calculated as

$$f_{dam}=\sum_{i\in\Omega} p(D_i)\cdot v_i \quad \text{(Eq. 2)}$$

where the sum is extended over all bins in the total-lung dose volume histogram, Ω, v_i is the fraction of the total lung volume in bin number *i*, D_i is the dose in that bin and $p(D_i)$ is the probability of local damage as given by Eq. 1. The probability of grade 3+ pneumonitis as a function of f_{dam} was read off the graphs published in Yorke 2005 derived from fitting the model described here to clinical data from the Memorial Sloan Kettering Cancer Center lung dose escalation trial.

RESULTS

Figure 3 shows the resulting treatment plan that we obtained in this way, and the dose to the entire lung volume, the VV and the total lung volume minus the VV are shown separately. One can clearly see from Figure 3 that the dose volume histogram for both lungs lies between the dose volume histogram for the VV and the dose volume histogram for the remaining lung volume. Quantitative analysis of these dose volume histograms yields the following NTD_{mean} values: VV NTD_{mean} = 9.94 Gy_3, lung NTD_{mean} = 12.5 Gy_3, and remaining lung volume NTD_{mean} = 16.69 Gy_3. This clearly shows that one can preferentially spare parts of the lung while still being able to keep the mean dose to the entire lung below the threshold dose for increased radiation pneumonitis of higher than grade 2. For comparison, a conventional treatment plan for this patient was then generated using the residual lung as the organ at risk. The plan was designed such that the resulting DVH for the residual lung was similar to that obtained for the case when differentially sparing the VV. As one can see from Figure 4, the DVH for the VV is now tracking that of the residual lung, while the DVH for the remaining lung is improved in the low dose and intermediate dose range but worsens in the high dose range, this is also borne out in the expected NTD_{mean} for these volumes, the NTD_{mean} for the VV increases by 3.58 Gy_3 to 13.52 Gy_3 while the the NTD_{mean} for the entire lung increases by only 1.45 Gy_3 to 13.95 Gy_3, and the NTD_{mean} for the remaining lung volume increases by 2.47 Gy_3 to an NTD_{mean} = 19.16 Gy_3.

Next, the parallel architecture model for grade 3+ pneumonitis with parameter values derived from clinical data sets were applied to the dose volume histograms from plans with and without sparing of the ventilated lung volume. Table 1 shows that sparing the VV more than halves the risk of grade 3+ pneumonitis relative to a plan without sparing of the VV. This calculation assumes that radiation injury in the fractional lung volume that is not ventilated at presentation, will not contribute to symptomatic pneumonitis.

DISCUSSION

Three primary research avenues seek to improve treatment outcome by optimizing the radiation dose distribution in NSCLC. First is the development of improved radiation delivery technology such as intensity modulated radiation therapy (IMRT) and image guided radiation therapy (IGRT), which may allow clinicians to safely decrease the margins required for target coverage and respiratory motion management. The second avenue attempts to improve target selection and delineation to reduce treatment volumes without compromising tumor control. Much interest is currently being devoted to the impact of multi-modality imaging, in particular CT-PET, in this context [22,23], but attention to microscopic patterns of spread and patterns of nodal spread remains critical in this endeavor. The third avenue aims to improve the therapeutic ratio through an optimization of the dose distribution in the normal lung tissue.

There are a wealth of data in the literature regarding dose-volume factors as predictors of pulmonary toxicity [24–26], and contemporary efforts at dose escalation frequently evaluate these parameters in an attempt to prospectively validate them [27]. One limitation of dose-volume analysis, which is perhaps under-appreciated, is the definition of the lung volumes themselves, specifically as it pertains to functional versus nonfunctional subvolumes. This fact is well appreciated by thoracic surgeons, who will routinely obtain lung scintigraphy scans to elucidate the contribution of a particular area of lung to overall pulmonary function[28], and also utilize the concept of “volume reduction” surgery in patients with severe emphysema to deliberately remove non-ventilating lung, and improve the ventilation-perfusion ratio. However, it is often overlooked by radiation oncologists, who will use the available data on normal tissue complication probability (NTCP) to guide them in design of a treatment plan, without recognizing that one of the fundamental premises of these models, “that all lung is

created equal," is erroneous. In fact, the differential contribution of different areas of lung tissue to overall pulmonary function has two major implications to the treatment planning process; one, that areas which are highly active in gas exchange should be spared to the maximum extent possible, and two, that areas which are functionally inactive or minimally active may potentially be exploited as "dead space", allowing escalation of dose through these already non- or minimally ventilatory areas. This concept is being increasingly recognized as a potentially significant one, and efforts at integrating this functional information are now appearing in the literature.[29]

While direct estimation of pneumonitis risk in a specific patient from published NTCP model parameters may not be very reliable, the estimated relative change in risk resulting from the various dose distributions in this study is probably more robust. In line with other authors [19–21,30], we feel that the parallel architecture model reflects the pathophysiology of symptomatic pneumonitis more closely than other models, such as the mean dose model or the Lyman-Kutcher-Burman model. The model parameters we used in this study have been applied in previous clinical outcome studies and have been found to produce clinically meaningful stratification of patients and dose plans into risk groups. The absolute reduction in the risk of symptomatic pneumonitis estimated here, in the order of 8 percentage points, may seem relatively modest. However, it should be noted that we are operating in the region of the relatively shallow foot of the sigmoid curve linking f_{dam} with complication risk. Clearly, in a higher-risk situation, we would expect a larger absolute risk reduction. The observed changes provide an important proof-of-principle but may also prove sufficient to allow the addition of concurrent chemotherapy or use of hypofractionated radiation schedules.

This remains a work in progress. We currently have several clinical protocols developing this technique as a potential tool to enhance radiotherapy delivery in lung cancer, and recognize that several limitations exist. First, we are generating plans based on a single time point HPH-MRI, and the ventilatory-competent lung volumes are likely to change over time. We clearly recognize this as a limitation; however, when a patient is seen in the clinic with a specific set of pulmonary function values and an HPH-MRI is obtained concurrently, one can be reasonably certain that depositing the highest doses of radiation to the least or non-ventilatory lung would have a high likelihood of leaving that patient with overall ventilatory capacity similar to that observed at baseline; in other words the patient is not very likely to be significantly "worse-off". In central tumors, where considerable atelectasis exists, re-aeration may occur and this could require replanning with a repeat HPH-MRI; the advantage of integrating treatment delivery using the conformal avoidance IMRT/IGRT paradigm is that the daily imaging inherent with cone-beam or MVCT would detect such re-aeration, thereby permitting timely replanning. Second, the use of simple thresholding to identify ventilated lung volume represents a first iteration of what is undoubtedly a complex process, which is dependent upon factors such as gravity-dependent variations in ventilation in the anterior to posterior direction for the supine patient position as well as variations in the sensitivity of the rf-coil used to detect the MRI signal. Future work is refining both the automated algorithm used to detect the ventilated space in the lungs using regional algorithms, as well as improving the rf-coil homogeneity for thoracic lung imaging. Third, HPH-MRI only provides ventilatory information and does not integrate perfusion information; it is possible in extreme cases to produce a ventilation-perfusion mismatch which could actually compromise a patient's lung function. Methods to assess perfusion with MR are currently in development, and could address this limitation in the future. Finally, the ultimate limitation is actually integrating this in a clinical trial and studying outcomes prospectively.

CONCLUSION

In summary, we believe that the functional information generated by HPH-MRI may have significant value in radiation treatment planning for NSCLC, allowing clinicians to improve the therapeutic ratio by selective avoidance of lung tissue which is maximally contributing to the patient's overall pulmonary function. A prospective feasibility study is currently in the process of development at the University of Wisconsin. It is our hope that this functional image guidance technique will ultimately allow us to positively impact outcomes in patients with this challenging disease.

References

1. Martel MK, Ten Haken RK, Hazuka MB, et al. Estimation of tumor control probability model parameters from 3-D dose distributions of non-small cell lung cancer patients. Lung Cancer 1999;24:31–7. [PubMed: 10403692]
2. Perez CA, Stanley K, Rubin P, et al. A prospective randomized study of various irradiation doses and fractionation schedules in the treatment of inoperable non-oat-cell carcinoma of the lung. Preliminary report by the Radiation Therapy Oncology Group. Cancer 1980;45:2744–53. [PubMed: 6991092]
3. Bentzen SM. Preventing or reducing late side effects of radiation therapy: radiobiology meets molecular pathology. Nat Rev Cancer 2006;6:702–13. [PubMed: 16929324]
4. Huang SM, Harari PM. Modulation of radiation response after epidermal growth factor receptor blockade in squamous cell carcinomas: inhibition of damage repair, cell cycle kinetics, and tumor angiogenesis. Clin Cancer Res 2000;6:2166–74. [PubMed: 10873065]
5. Gandara DR, Chansky K, Albain KS, et al. Long-term survival with concurrent chemoradiation therapy followed by consolidation docetaxel in stage IIIB non-small-cell lung cancer: a phase II Southwest Oncology Group Study (S9504). Clin Lung Cancer 2006;8:116–21. [PubMed: 17026812]
6. Cox JD, Azarnia N, Byhardt RW, et al. A randomized phase I/II trial of hyperfractionated radiation therapy with total doses of 60.0 Gy to 79.2 Gy: possible survival benefit with greater than or equal to 69.6 Gy in favorable patients with Radiation Therapy Oncology Group stage III non-small-cell lung carcinoma: report of Radiation Therapy Oncology Group 83-11. J Clin Oncol 1990;8:1543–55. [PubMed: 2167952]
7. Saunders M, Dische S, Barrett A, et al. Continuous, hyperfractionated, accelerated radiotherapy (CHART) versus conventional radiotherapy in non-small cell lung cancer: mature data from the randomised multicentre trial. CHART Steering committee. Radiother Oncol 1999;52:137–48. [PubMed: 10577699]
8. Nagata Y, Takayama K, Matsuo Y, et al. Clinical outcomes of a phase I/II study of 48 Gy of stereotactic body radiotherapy in 4 fractions for primary lung cancer using a stereotactic body frame. Int J Radiat Oncol Biol Phys 2005;63:1427–31. [PubMed: 16169670]
9. Hoyer M, Roed H, Hansen AT, et al. Prospective study on stereotactic radiotherapy of limited-stage non-small-cell lung cancer. Int J Radiat Oncol Biol Phys 2006;66:S128–35.
10. Timmerman R, McGarry R, Yiannoutsos C, et al. Excessive toxicity when treating central tumors in a phase II study of stereotactic body radiation therapy for medically inoperable early-stage lung cancer. J Clin Oncol 2006;24:4833–9. [PubMed: 17050868]
11. McGuire SM, Zhou S, Marks LB, et al. A methodology for using SPECT to reduce intensity-modulated radiation therapy (IMRT) dose to functioning lung. Int J Radiat Oncol Biol Phys 2006;66:1543–52. [PubMed: 17126212]
12. Christian JA, Partridge M, Nioutsikou E, et al. The incorporation of SPECT functional lung imaging into inverse radiotherapy planning for non-small cell lung cancer. Radiother Oncol 2005;77:271–7. [PubMed: 16274762]
13. Seppenwoolde Y, Engelsman M, De Jaeger K, et al. Optimizing radiation treatment plans for lung cancer using lung perfusion information. Radiother Oncol 2002;63:165–77. [PubMed: 12063006]
14. Kauczor HU, Hofmann D, Kreitner KF, et al. Normal and abnormal pulmonary ventilation: visualization at hyperpolarized He-3 MR imaging. Radiology 1996;201:564–8. [PubMed: 8888259]

15. Musch G, Venegas JG. Positron emission tomography imaging of regional lung function. Minerva Anestesiol 2006;72:363–7. [PubMed: 16682902]

16. de Lange EE, Altes TA, Patrie JT, et al. Evaluation of asthma with hyperpolarized helium-3 MRI: correlation with clinical severity and spirometry. Chest 2006;130:1055–62. [PubMed: 17035438]

17. Fain SB, Panth SR, Evans MD, et al. Early emphysematous changes in asymptomatic smokers: detection with 3He MR imaging. Radiology 2006;239:875–83. [PubMed: 16714465]

18. Ireland RH, Bragg CM, McJury M, et al. Feasibility of image registration and intensity-modulated radiotherapy planning with hyperpolarized helium-3 magnetic resonance imaging for non-small-cell lung cancer. Int J Radiat Oncol Biol Phys 2007;68:273–81. [PubMed: 17448880]

19. Withers HR, Taylor JM, Maciejewski B. Treatment volume and tissue tolerance. Int J Radiat Oncol Biol Phys 1988;14:751–9. [PubMed: 3350731]

20. Yorke ED, Jackson A, Rosenzweig KE, et al. Dose-volume factors contributing to the incidence of radiation pneumonitis in non-small-cell lung cancer patients treated with three-dimensional conformal radiation therapy. Int J Radiat Oncol Biol Phys 2002;54:329–39. [PubMed: 12243805]

21. Yorke ED, Jackson A, Rosenzweig KE, et al. Correlation of dosimetric factors and radiation pneumonitis for non-small-cell lung cancer patients in a recently completed dose escalation study. Int J Radiat Oncol Biol Phys 2005;63:672–82. [PubMed: 15939548]

22. Deniaud-Alexandre E, Touboul E, Lerouge D, et al. Impact of computed tomography and 18F-deoxyglucose coincidence detection emission tomography image fusion for optimization of conformal radiotherapy in non-small-cell lung cancer. Int J Radiat Oncol Biol Phys 2005;63:1432–41. [PubMed: 16125870]

23. Grills IS, Yan D, Black QC, et al. Clinical implications of defining the gross tumor volume with combination of CT and (18)FDG-positron emission tomography in non-small-cell lung cancer. Int J Radiat Oncol Biol Phys 2007;67:709–19. [PubMed: 17197120]

24. Kwa SL, Lebesque JV, Theuws JC, et al. Radiation pneumonitis as a function of mean lung dose: an analysis of pooled data of 540 patients. Int J Radiat Oncol Biol Phys 1998;42:1–9. [PubMed: 9747813]

25. Hernando ML, Marks LB, Bentel GC, et al. Radiation-induced pulmonary toxicity: a dose-volume histogram analysis in 201 patients with lung cancer. Int J Radiat Oncol Biol Phys 2001;51:650–9. [PubMed: 11597805]

26. Kocak Z, Borst GR, Zeng J, et al. Prospective assessment of dosimetric/physiologic-based models for predicting radiation pneumonitis. Int J Radiat Oncol Biol Phys 2007;67:178–86. [PubMed: 17189069]

27. Bradley J, Graham MV, Winter K, et al. Toxicity and outcome results of RTOG 9311: a phase I-II dose-escalation study using three-dimensional conformal radiotherapy in patients with inoperable non-small-cell lung carcinoma. Int J Radiat Oncol Biol Phys 2005;61:318–28. [PubMed: 15667949]

28. Larsen KR, Lund JO, Svendsen UG, et al. Prediction of post-operative cardiopulmonary function using perfusion scintigraphy in patients with bronchogenic carcinoma. Clin Physiol 1997;17:257–67. [PubMed: 9171966]

29. Yaremko BP, Guerrero TM, Noyola-Martinez J, et al. Reduction of normal lung irradiation in locally advanced non-small-cell lung cancer patients, using ventilation images for functional avoidance. Int J Radiat Oncol Biol Phys 2007;68:562–71. [PubMed: 17398028]

30. Jackson A, Kutcher GJ, Yorke ED. Probability of radiation-induced complications for normal tissues with parallel architecture subject to non-uniform irradiation. Med Phys 1993;20:613–25. [PubMed: 8350812]

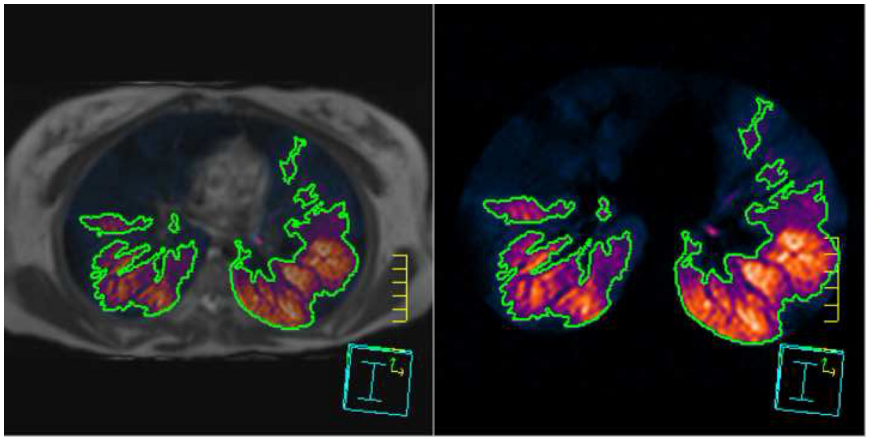

Figure 1.
Shown on the right is the auto segmentation of the most prominent areas active in gas exchange on the HPH-MRI data set. Shown on the left is cross correlation of the HPH-MRI to a proton density weighted (PD_w) MRI obtained during the same imaging session to yield anatomical detail.

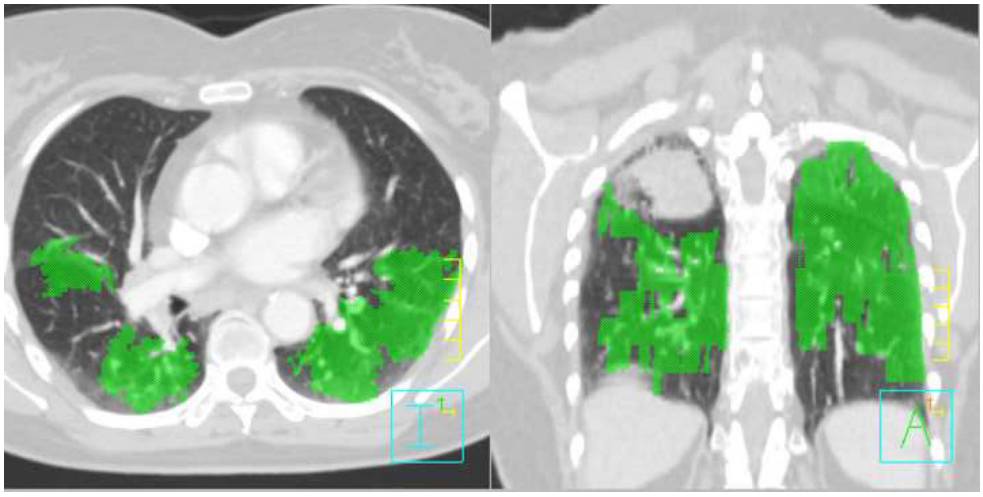

Figure 2.
The areas shown in green color wash signify areas that are active in gas exchange that have been projected onto the treatment planning CT from the HPH-MRI data set.

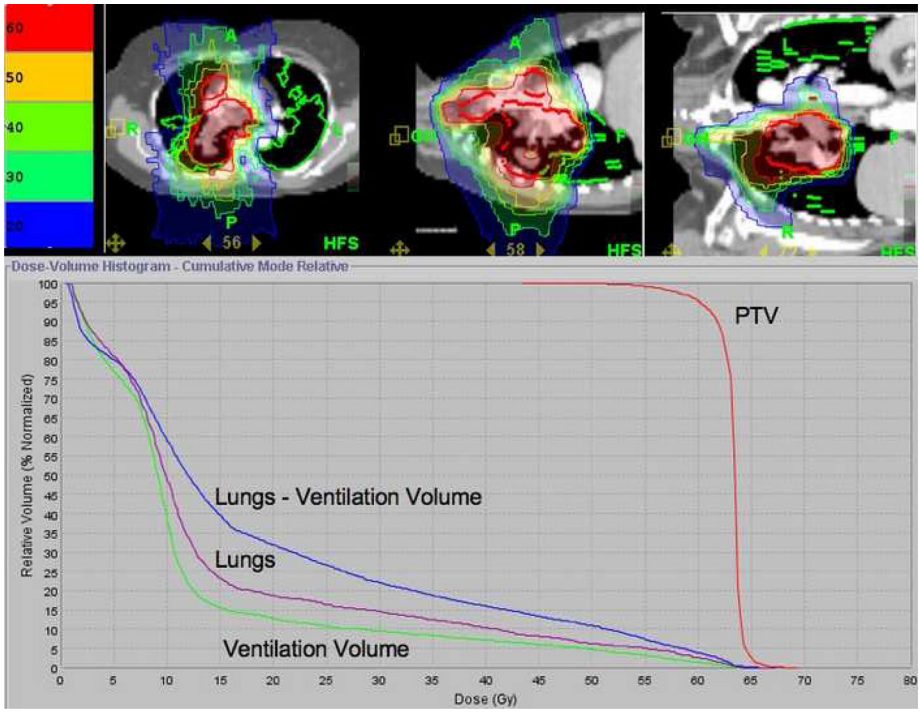

Figure 3.
Tomotherapy Treatment plan in which different volumes of the lungs were spared differentially based on the their prominence in the gas exchange.

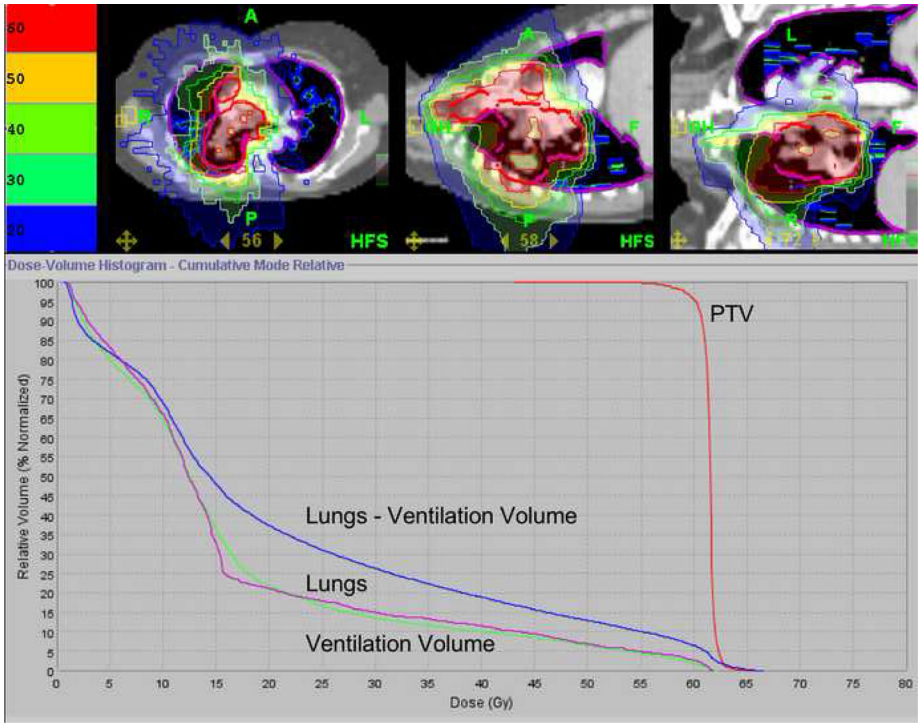

Figure 4.
Conventional Lung Tomotherapy Treatment plan in which the residual healthy lung is taken as the organ at risk.

Table 1

Calculated risk of grade 3+ pneumonitis in the conventional versus functionally optimized plan.

		Fraction of damaged subunits, f_{dam}	**Grade 3+ pneumonitis, parameters from [20]**
Conventional plan	Ventilated lung	0.24	12%
Functionally optimized plan	Ventilated lung	0.15	4%
	Residual lung*	(0.29)	(22%)

*It is hypothesized here, that damage to non-ventilated lung will not contribute to the risk of symptomatic pneumonitis. Risk estimate given for comparison only.